THE JOURNAL OF PHYSICAL CHEMISTRY C
A JOURNAL OF THE AMERICAN CHEMICAL SOCIETY

pubs.acs.org/JPCC

Article

Passivating Deep-Level Defects with Ag Alloying to Enhance the Efficiency of $Cu(In,Ga)(S,Se)_2$ Solar Cells

Xuan-Yan Chen, Zihan Huang, Zecheng Gan, Baoying Dou, Yan Wang, Xie Zhang,* and Chang Yan*

Cite This: https://doi.org/10.1021/acs.jpcc.5c02431

Read Online

ACCESS | Metrics & More | Article Recommendations

ABSTRACT: Chalcopyrite $Cu(In,Ga)(S,Se)_2$ is one of the most promising photovoltaic candidates, presenting huge potential in future flexible and tandem solar cell applications. Ag alloying was recognized as an effective strategy to improve the efficiency of selenide $Cu(In,Ga)Se_2$ solar cells, enabling record efficiencies. However, the fundamental mechanism underlying these remarkable performance enhancements remains elusive; especially, how Ag alloying alters the properties of point defects and the corresponding nonradiative recombination is still unclear. Here, we perform rigorous first-principles calculations to systematically investigate the native point defects in $CuInSe_2$ and $CuInS_2$ in comparison with those in $AgInSe_2$ and $AgInS_2$. We find that anion vacancies are critical deep-level defects that may act as nonradiative recombination centers, limiting the photovoltaic performance. We show that Ag alloying can effectively passivate these deep-level defects in both $CuInSe_2$ and $CuInS_2$, shallowing their charge−state transition levels, which is due to a band gap widening effect as a result of lattice expansion induced by Ag alloying; this beneficial effect is more pronounced in $CuInS_2$ than in $CuInSe_2$, which has been further verified by experiments on $Cu(In,Ga)S_2$ solar cells with and without Ag alloying. Our insights will guide the optimization and design of $Cu(In,Ga)(S,Se)_2$-based solar cells, pushing their performance toward the Shockley−Queisser limit.

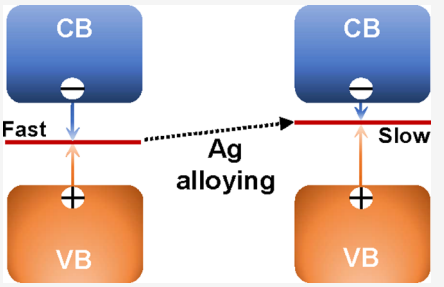

1. INTRODUCTION

Chalcopyrite $Cu(In,Ga)(S,Se)_2$-based solar cells have shown remarkable potential in the field of flexible and tandem photovoltaics due to their favorable optoelectronic properties, high efficiency, lightweight nature, and tunable band gap. Early developments in $Cu(In,Ga)(S,Se)_2$ solar cells focused on the introduction of various compositional and structural modifications to improve the photovoltaic efficiency, such as compositional grading within the absorber layer[1,2] and alkali metal postdeposition treatments.[3−7] These strategies have gradually increased the power conversion efficiencies of $Cu(In,Ga)(S,Se)_2$ solar cells to be greater than 20%.[4,8]

Recently, alloying $Cu(In,Ga)Se_2$(CIGSe) with Ag was found to be an effective approach to further enhance the power conversion efficiency, contributing to the recent record (23.6%) efficiency.[9] The effectiveness of this approach was well-recognized. However, the underlying mechanism is still unclear. Some researchers attributed the enhancement to the fact that Ag alloying can effectively enlarge the grain size and large grain facilitates the carrier transport.[10,11] Others ascribed the enhancement to band-structure change in which Ag alloying lowers the valence-band maximum (VBM), thus reducing the interface recombination by enhancing the interface injection recombination barrier. Nevertheless, the carrier recombination is intimately related to the point defects in the CIGSe layer; however, the defects that act as nonradiative recombination centers are still unclear. Therefore, elucidating the chemical nature of the point defect of chalcogenide before and after Ag alloying is interesting and of great significance for understanding the role of Ag alloying for CIGSe.

In order to throw light upon this issue, we perform accurate first-principles calculations using the Heyd-Scuseria-Ernzerhof (HSE)[12] hybrid functional (which gives a better description of the band gap compared to (semi)local exchange−correlation functionals[13]) to systematically evaluate the native point defects in $CuIn(S,Se)_2$ in comparison with those in $AgIn(S,Se)_2$. It has been reported in the literature[14−18] that defect clusters are relevant for CIGSe. But, we note that they usually become critical in heavily doped semiconductors[15] or at the $Cu(In,Ga)Se_2$/buffer interface and line/planar defects.[18] In this work, we focus on the situation with dilute defect concentrations where defect clusters are less likely to form. We find that anion vacancies are deep-level defects in $CuIn(S,Se)_2$, which may mediate strong nonradiative recombination. Ag alloying effectively passivates the anion vacancies by shifting

Received: April 9, 2025
Revised: April 20, 2025
Accepted: April 21, 2025

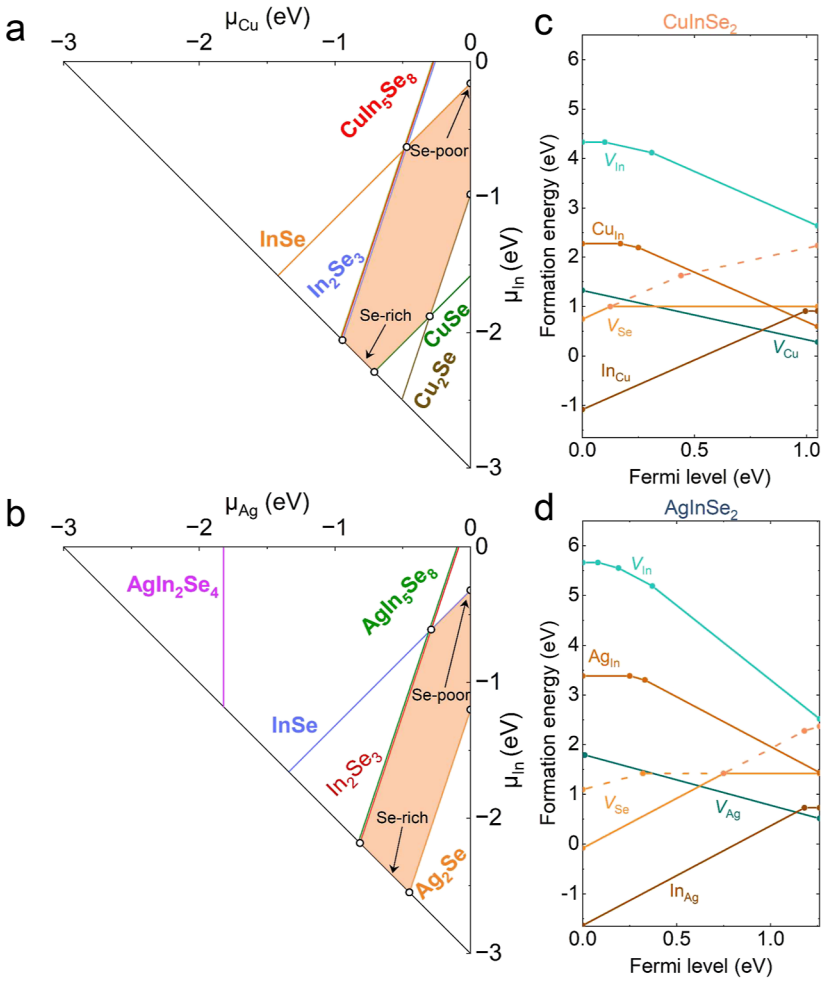

Figure 1. Thermodynamic stability of (a) $CuInSe_2$ and (b) $AgInSe_2$ as a function of the chemical potentials. Formation energies of the native point defects in (c) $CuInSe_2$ and (d) $AgInSe_2$ as a function of the Fermi level for Se-poor synthesis conditions, as determined in panels (a,b), respectively.

the (2+/+) transition level from midgap toward the conduction-band minimum (CBM), becoming a shallow level. The introduction of Ag with a larger radius leads to an expansion of the CuIn X_2 lattice, which causes the VBM and CBM to move toward lower energy levels simultaneously. However, the energy reduction of the VBM (characterized by *p-d* coupling) is greater than that of the CBM, which is an antibonding state between S/Se *p* and In *s*; these shifts result in an increase in the band gaps, converting deep-level anion vacancies to shallower ones. In addition, Ag alloying in $CuInS_2$ will not introduce a new transition level approaching midgap like $CuInSe_2$, which makes it more efficient to enhance the V_{oc} in $Cu(In,Ga)S_2$ cells. In this way, Ag can effectively mitigate the nonradiative losses caused by the anion vacancies. This insight reveals how Ag alloying reduces the nonradiative recombination and enhances the power conversion efficiency from the perspective of point defects, which is critical for understanding and further improving the performance of $Cu(In,Ga)(S,Se)_2$ materials and devices.

2. METHODS

All first-principles calculations in this work are based on the density functional theory using the HSE hybrid functional.[12] We use project augmented-wave pseudopotentials[19] as implemented in the Vienna ab initio simulation package (VASP).[20] A plane-wave energy cutoff of 400 eV and a 1 × 1 × 1 Monkhorst−Pack[21] *k*-point grid are used for the supercells of $CuInS_2$, $AgInS_2$, $CuInSe_2$, and $AgInSe_2$ with 288 atoms. In our work, we consistently perform HSE relaxations for all defect configurations. Using a mixing parameter of 0.29 for the HSE functional, we obtain band gaps of 1.5 eV for $CuInS_2$, 1.86 eV for $AgInS_2$, 1.05 eV for $CuInSe_2$, and 1.26 eV for $AgInSe_2$, in good agreement with the experiment.[22−24]

Taking $CuInS_2$ as an example, we illustrate how the chemical potentials are determined. When $CuInS_2$ is formed as a stable phase, the chemical potentials of the host species should follow

$$\mu_{Cu} + \mu_{In} + 2\mu_S = \Delta H^f(CuInS_2) = -2.52 \text{ eV} \quad (1)$$

where $\Delta H^f(CuInS_2)$ is the formation enthalpy of $CuInS_2$ calculated from first principles. The chemical potentials are referenced to the calculated energies of the pure bulk species. The formation enthalpies of the competing phase (CuS, Cu_2S and CuS_2 etc.) provide additional bounds to the chemical potentials, that is

$$\mu_{Cu} + \mu_S < \Delta H^f(CuS) = -0.51 \text{ eV} \quad (2)$$

$$2\mu_{Cu} + \mu_S < \Delta H^f(Cu_2S) = -0.88 \text{ eV} \quad (3)$$

$$\mu_{Cu} + 2\mu_S < \Delta H^f(CuS_2) = -0.20 \text{ eV} \quad (4)$$

https://doi.org/10.1021/acs.jpcc.5c02431
J. Phys. Chem. C XXXX, XXX, XXX−XXX

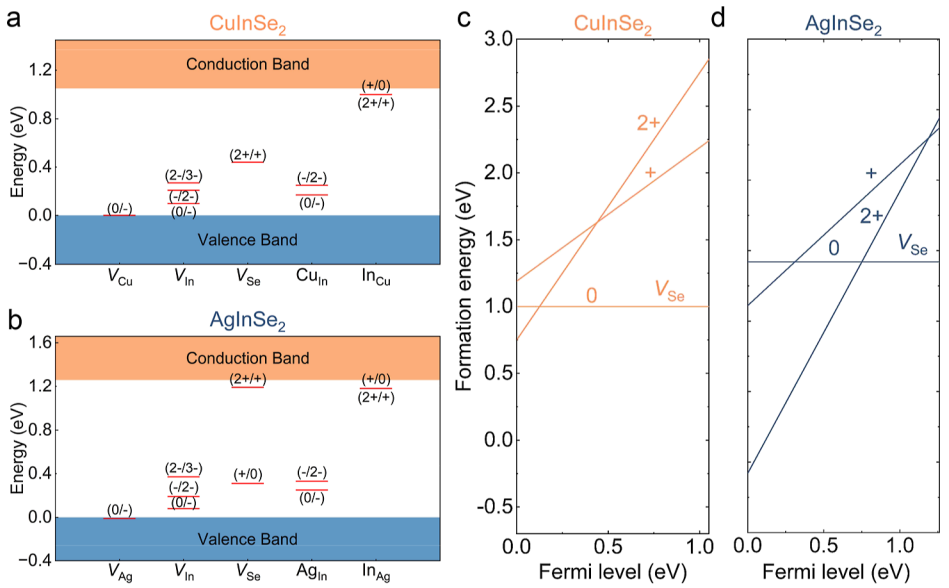

Figure 2. Charge-state transition levels of intrinsic defects in (a) $CuInSe_2$ and (b) $AgInSe_2$. Formation energy of V_{Se} as a function of the Fermi level in (c) $CuInSe_2$ and (d) $AgInSe_2$.

With eqs 1−4, we can determine the phase diagram and bounds of μ_{Cu} and μ_{In}, as shown in Figure 1a.

The formation energy (E^f) of a point defect D with charge state q is given by[25]

$$E^f(D^q) = E_{tot}(D^q) - E_{tot}(\text{bulk}) - \sum_i n_i\mu_i + qE_F + \Delta^q \quad (5)$$

where $E_{tot}(D^q)$ is the total energy of a supercell of $CuInS_2$ containing the defect D in charge state q. $E_{tot}(\text{bulk})$ is the total energy of the pristine $CuInS_2$ supercell with 288 atoms. The parameter n_i is the number of atomic species i added to ($n_i > 0$) or removed from ($n_i < 0$) the supercell to create the defect D; μ_i is the chemical potential of atomic species i; E_F is the Fermi level (the chemical potential of electrons) referenced to the VBM; Δ^q is a finite-size correction term for charged defects.[26]

Metal precursors with a thickness of approximately 600 nm are prepared by cosputtering either CuGa (atom ratio: 70% Cu, 30% Ga) or CuAgGa (atom ratio: 56% Cu, 14% Ag, 30% Ga) targets onto Mo-coated glass substrates using a magnetron sputtering system. The samples are then subjected to a prealloying process at around 150 °C and then transferred to a rapid thermal processing (AS-One 100) to anneal at 600 °C for several minutes in a sulfur atmosphere with a ramping rate of 60 °C/min. The details of CdS deposition can be found in ref 27. After that, a window layer consisting of 50 nm high-resistant zinc oxide and 240 nm indium tin oxide (ITO) with a sheet resistance below 30 Ω/sq is deposited via sputtering. Finally, metal grids are thermally evaporated as the top contact, and the total area of the fabricated cells is defined as around 0.1 cm^2 through mechanical scribing.

3. RESULTS AND DISCUSSION

It has been shown in the existing literature[28] that the defect formation energies in $CuGaSe_2/CuGaS_2$ are similar to those in $CuInSe_2/CuInS_2$. This trend applies to the transition levels as well. To make our computational modeling more tractable, we focus on In-based compounds without Ga alloying. Hence, in the present study, we assess the defect properties in both $CuInSe_2$ and $CuInS_2$.

We first evaluate the thermodynamic stability of selenide chalcopyrite $CuInSe_2$ as a function of the chemical potentials of Cu (μ_{Cu}) and In (μ_{In}), as shown in Figure 1a. $CuInSe_2$ is stable in the orange-shaded region against decomposition or transformation into its competing phases, which allows us to determine the bounds of the chemical potentials. We mainly focus on the set of chemical potentials marked "Se-poor" in Figure 1a, which corresponds to the equilibrium limits of the experimental synthesis conditions.

Using the chemical potentials determined, we calculate the formation energies of the native point defects in $CuInSe_2$, including two antisite defects (Cu_{In} and In_{Cu}) and three vacancies (V_{Cu}, V_{In}, and V_{Se}) as depicted in Figure 1c. We found from the literature[28−30] that the interstitial defects (e.g., Cu_i) in these materials are shallow,[28] unlikely to cause recombination losses. Hence, we exclude the interstitial defects from our present study. Meanwhile, we noticed that V_{Cu}, $V_{(In,Ga)}$, and two antisite defects have been frequently studied,[31] but the anion vacancy V_{Se} has been rarely investigated for its high formation energy.[31] Thereby, we pay particular attention to the formation energies and transition levels of anion vacancies to assess their impacts on efficiency. Under Se-poor conditions, V_{In} has the highest formation energy: the formation energy of V_{In}^0 is 4.4 eV, followed by Cu_{In} and then V_{Cu}. This is because the chemical potentials of Cu and In are high under Se-poor conditions. Compared with the other three defects, V_{Se} and In_{Cu} have relatively low formation energies. The formation energy of V_{Se}^0 is only 1.0 eV, which means that under Se-poor conditions, V_{Se} is particularly easy to form.

In order to investigate the impact of Ag alloying on the formation energy of native point defects in $CuInSe_2$, we substitute Cu with Ag in $CuInSe_2$ and then calculate the formation energies of defects in $AgInSe_2$. As shown in Figure 1d, there are two interesting observations: (i) After the incorporation of Ag, the overall formation energies of these five kinds of point defects increase, which means that the incorporation of Ag could reduce the defect concentrations;

https://doi.org/10.1021/acs.jpcc.5c02431
J. Phys. Chem. C XXXX, XXX, XXX−XXX

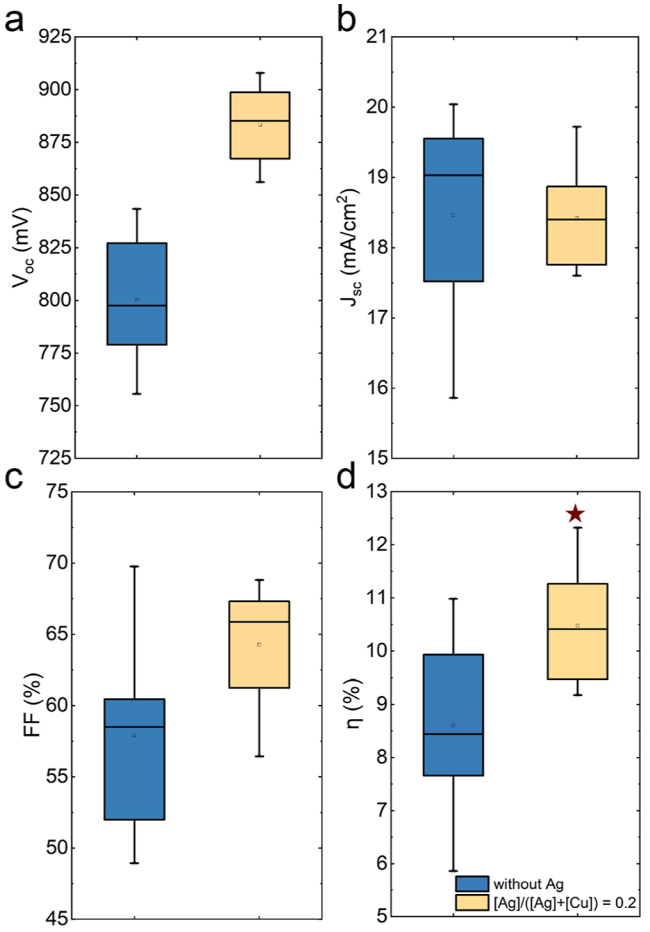

Figure 3. Statistical box plot of device performance parameters for $Cu(In,Ga)S_2$ solar cells with and without Ag alloying. The ratio of Ag alloying is [Ag]/([Ag]+[Cu]) = 0.2. The box plot denotes median (central line), mean value (dots), 25th percentile (bottom edge of the box), 75th percentile (top edge of the box), 95th percentile (upper whisker), and fifth percentile (lower whisker). The sample size in each column is 8 devices. The red star denotes the efficiency of the champion cell.

(ii) the order of formation energies of the five types of defects is consistent with that in $CuInSe_2$, but the positions of the transition levels are altered, especially those of V_{Se}.

In addition to the impact on the formation energies of point defects in $CuInSe_2$, the introduction of Ag also changes the relative position of the transition levels in the band gap. To intuitively probe the changes of the transition levels in $CuInSe_2$, we summarize all the transition levels within the band gap in Figure 2a. To act as a nonradiative recombination center, a prerequisite is that the defect has charge−state transition levels in the band gap.[32,33] In addition, it is highly unlikely that defects capture two electrons or two holes at once. As a result, charge−state transition levels between nonadjacent charge states such as (2+/0) is not active for nonradiative recombination.[34] For V_{Cu} in $CuInSe_2$, there is a (0/−) transition level but not within the band gap (located at the VBM). Therefore, V_{Cu} cannot be a nonradiative recombination center in $CuInSe_2$. In the case of V_{In}, the formation energy of V_{In} is so high under Se-poor and In-rich conditions that it is difficult to form, which is thus not critical. It is noteworthy that V_{Se} has a (2+/+) transition level in the band gap. Moreover, the (2+/+) transition level is deep in the band gap, which means that V_{Se} may efficiently capture electrons and holes, simultaneously. V_{Se} is potentially an efficient nonradiative recombination center. As for the two antisite defects, Cu_{In} has a relatively deep (−/2−) transition level within the band gap. Both the (+/0) and (2+/+) transition levels of In_{Cu} are very close to the CBM. In_{Cu} is highly unlikely to be an efficient nonradiative recombination center.

To investigate the effect of Ag alloying on the transition levels of the five defects within the band gap, we plot the transition levels of $AgInSe_2$ in Figure 2b. Other than the (2+/+) transition level of V_{Se}, the relative positions of the transition levels of the other four defects within the band gap do not change significantly. It is noteworthy that the (2+/+) transition level of V_{Se} shifts from 0.44 eV above the VBM in $CuInSe_2$ to 0.07 eV below the CBM in $AgInSe_2$. The introduction of Ag causes V_{Se} to transform from a deep-level defect to a shallow one. It also increases the formation energy of V_{Se}, reducing the probability of V_{Se} generation and mitigating the negative impact of nonradiative recombination induced by V_{Se} on the efficiency of $CuInSe_2$ solar cells.

We note that Ag substitution introduces a new (+/0) transition level of V_{Se} in the band gap. The (+/0) transition level is 0.3 eV above the VBM in $AgInSe_2$. The corresponding (2+/+) transition level of V_{Se} in $CuInSe_2$ is 0.44 eV above the VBM. The difference in the absolute values does not seem to be that significant, but the band gaps of $CuInSe_2$ and $AgInSe_2$ are also different: 1.05 eV for $CuInSe_2$ and 1.26 eV for $AgInSe_2$. This means that the (2+/+) transition level is 0.61 eV below the CBM in $CuInSe_2$, and the (+/0) transition level is 0.96 eV below the CBM in $AgInSe_2$. It is highly unlikely for the (+/0) transition level to efficiently capture electrons from the CBM to complete a nonradiative recombination cycle, which means that the (+/0) transition has a very limited impact on the capture coefficient and device efficiency. Based on the discussion above, we can now better understand from the perspective of point defects why high-concentration Ag alloying can enhance the performance of $Cu(In,Ga)Se_2$ solar cells, enabling a certified efficiency of 23.64%.[9] High-concentration Ag alloying pushes the deep transition level of V_{Se} toward the band edge, suppressing the resulting nonradiative recombination. This is because replacing Cu with Ag in In-based chalcopyrites pushes the band edges to lower energies relative to vacuum, with the valence band undergoing a larger downward shift than the conduction band.[35,36] This is associated with the orbital character of the band edges and the strength of the *p-d* coupling. The CBM is an antibonding state between S/Se *p* and In *s*, while the VBM arises from an antibonding state between S/Se *p* and Cu/Ag *d*.[37] Due to the smaller radius of Cu compared to Ag, the lattice parameters increase when replacing Cu with Ag, thereby weakening the antibonding interaction and lowering the CBM and VBM simultaneously but with different extents. The downward shifts are smaller in the *s*-derived band than in the *p-d* derived band. These shifts lead to wider band gaps for both $AgInSe_2$ and $AgInS_2$ compared to their Cu counterparts. One positive outcome is that the deep-level anion vacancies in $CuInX_2$ (X = Se and S) become shallower in $AgInX_2$.

The promoting effect of Ag alloying on V_{oc} of CIGSe has already been reported in the literature.[10,38] With high-concentration Ag alloying, around [Ag]/([Ag]+[Cu]) = 0.2, the V_{oc} increased from 741 mV[39] to 767 mV[9] (i.e., by 26 mV). However, it is still unclear if Ag alloying can also enhance the

https://doi.org/10.1021/acs.jpcc.5c02431
J. Phys. Chem. C XXXX, XXX, XXX−XXX

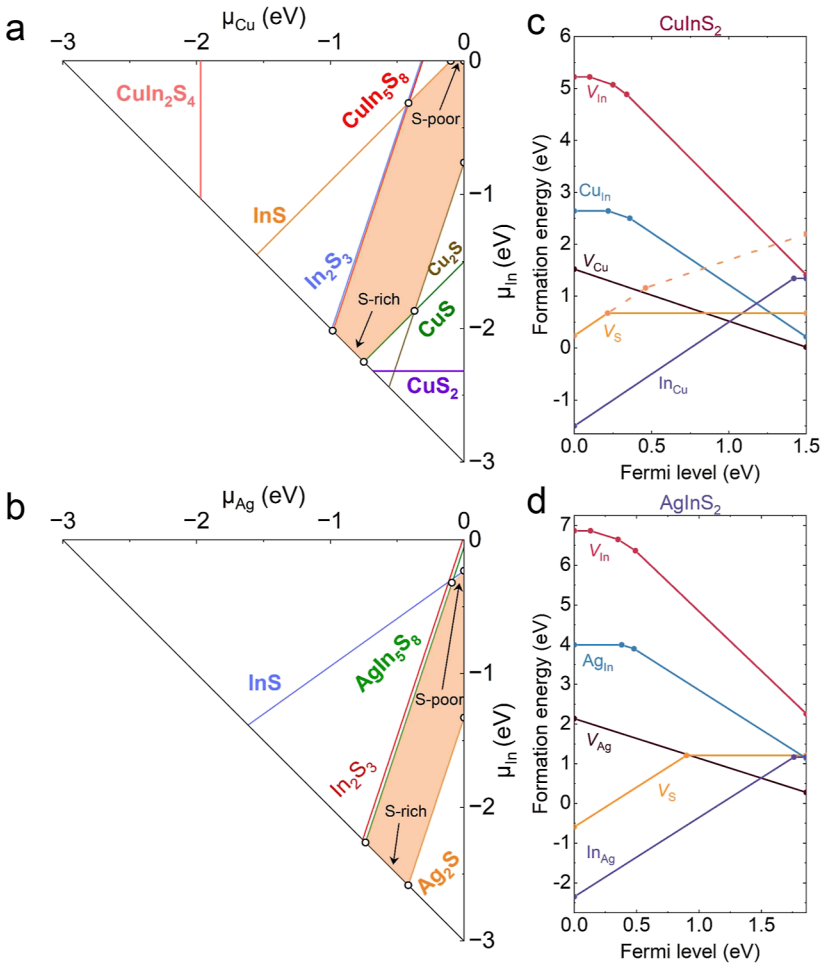

Figure 4. Thermodynamic stability of (a) $CuInS_2$ and (b) $AgInS_2$ as a function of the chemical potentials. Formation energies of the native point defects in (c) $CuInS_2$ and (d) $AgInS_2$ as a function of the Fermi level for S-poor synthesis conditions, as determined in (a,b), respectively.

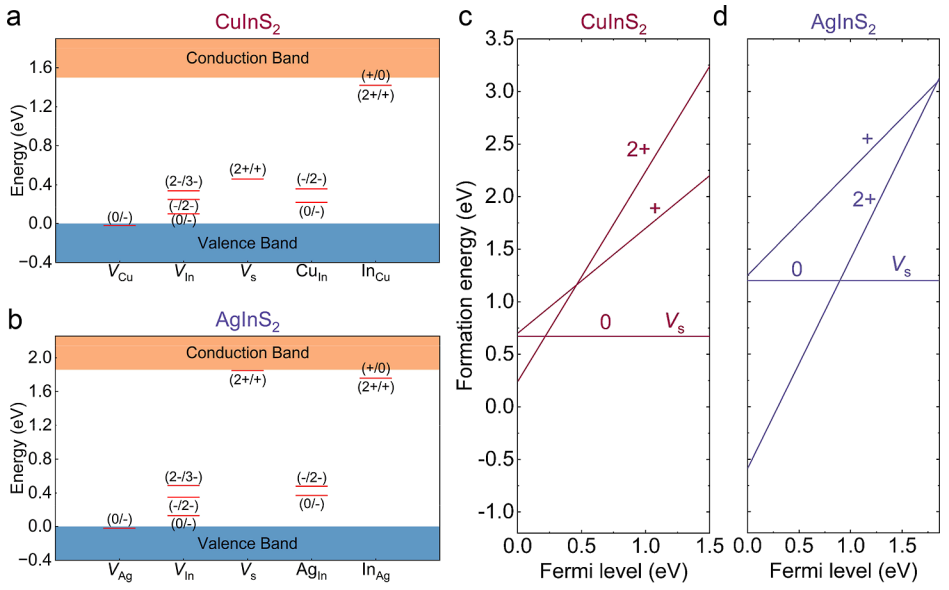

Figure 5. Charge-state transition levels of intrinsic defects in (a) $CuInS_2$ and (b) $AgInS_2$. Formation energy of V_S as a function of the Fermi level in (c) $CuInS_2$ and (d) $AgInS_2$.

V_{oc} of the sulfide-based solar cells and to what extent can V_{oc} be improved. Motivated by the observations in the $CuInSe_2$, the effectiveness of Ag alloying in the elevation of V_{oc} of CIGSe, we perform experiments[40] to investigate the impact of Ag alloying on the V_{oc} and photovoltaic performance of the wide-band gap sulfide Cu(In,Ga)S_2 (CIGSu) solar cell. After

https://doi.org/10.1021/acs.jpcc.5c02431
J. Phys. Chem. C XXXX, XXX, XXX−XXX

Ag alloying with an [Ag]/([Ag]+[Cu]) ratio of around 20%, the average efficiency increased from ~8.5% to over 10% [see Figure 3d]. The average V_{oc} of (Ag,Cu)(In,Ga)S_2 cells is significantly improved from ~800 to around 883 mV, with a notable increase of 83 mV. Our experimental results show that Ag alloying is an effective means to improve the efficiency of Cu(In,Ga)S_2 solar cells with the champion efficiency above 12.5%. However, the underlying mechanism is still unclear. How does Ag alloying affect the properties of point defects in CIGSu and thus change the V_{oc}? In particular, why does Ag alloying have an even more pronounced enhancement in the V_{oc} in CIGSu compared to that in CIGSe? These questions need to be answered.

Hence, we further examine how Ag alloying influences the formation energies of native point defects in $CuInS_2$. We employ the same approach to calculate the phase diagrams of $CuInS_2$ and $AgInS_2$ to determine the chemical potentials in the synthesis conditions. Similarly, under S-poor conditions, we calculate the formation energies of two antisite defects (Cu_{In} and In_{Cu}) and three vacancies (V_{Cu}, V_{In}, and V_S), as depicted in Figure 4c. Figure 4d shows the formation energies of the five kinds of point defects after Cu is replaced with Ag. The incorporation of Ag into $CuInS_2$ can also increase the overall formation energies of the defects. This means that Ag alloying could reduce the defect densities in both $CuInSe_2$ and $CuInS_2$.

$CuInS_2$ and $CuInSe_2$ share a similar structure with the same tetragonal phase in the *I*-42*d* space group. The only difference between them is the anion. Thereby, $CuInS_2$ and $CuInSe_2$ have similar defects, and the properties of these defects are also alike. As shown in Figure 5, the transition levels of the point defects in $CuInS_2$ have a distribution similar to that in $CuInSe_2$. The incorporation of Ag in $CuInS_2$ has a similar effect as the one in $CuInSe_2$. The relative positions of the transition levels of the two vacancies (V_{Ag} and V_{In}) and two antisites (Ag_{In} and In_{Ag}) within the band gap do not change much. In contrast, the introduction of Ag has a significant effect on the relative positions of the transition levels of V_S within the band gap. We can see from Figure 5a that there is only a (2+/+) transition level close to the midgap. However, after Ag-substitution, the (2+/+) transition level shifts from midgap in the $CuInS_2$ to 0.01 eV below the CBM in $AgInS_2$. The introduction of Ag makes the (2+/+) transition level of V_S in $CuInS_2$ become shallower than that in $CuInSe_2$, which can efficiently mitigate the nonradiative recombination caused by this transition.

Unlike the situation in $CuInSe_2$, the substitution of Ag for $CuInS_2$ does not introduce a new (+/0) transition level of V_S in the band gap. In other words, Ag alloying should have an even more pronounced positive effect on enhancing the efficiency of $CuInS_2$. This also has been demonstrated by the experimental results, in which the increase of V_{oc} in CIGSu is around three times higher than that of CIGSe, as we mentioned before. Ag alloying suppresses nonradiative recombination caused by anion vacancies, which serves as one of the key factors that enhance V_{oc} and efficiency by elongating the charge carrier lifetime and enhancing the carrier mobility.

The charge carrier lifetime, along with carrier mobility, defines the diffusion length, which reflects whether the photogenerated charge carrier can reach the respective electrode or not. Deep-level defects in CIGS, such as V_{Se} and V_S, are expected to decrease the charge carrier lifetime through nonradiative recombination.[41] Ag alloying pushes the transition level of the anion vacancies from midgap toward the CBM, meaning that the probability of anion vacancies capturing holes from the VBM will decrease. Thus, the total nonradiative recombination rate decreases, elongating the carrier lifetime. In addition, Ag alloying will expand the lattice, which decreases the coupling between charge carriers and defects, reducing the probability of carriers being scattered or trapped by defects.[42] The overall carrier mobility will thus be enhanced.

4. CONCLUSIONS

In summary, we have performed first-principles calculations to examine the native defects in chalcopyrite $CuInSe_2$ and $CuInS_2$, in comparison with those in $AgInSe_2$ and $AgInS_2$. We uncovered that V_S and V_{Se} are deep-level defects that may act as detrimental nonradiative recombination centers that can be effectively passivated by Ag alloying through shallowing of the transition levels. This is due to a band gap widening effect as a result of lattice expansion induced by Ag alloying. The passivation effect is stronger in $CuInS_2$ than in $CuInSe_2$, which has been experimentally verified in our fabricated devices with Ag alloyed Cu(In,Ga)S_2, showing significant V_{oc} enhancement. Our results suggest that to further enhance the performance of chalcopyrite Cu(In,Ga)(S,Se)$_2$ solar cells, future research should focus on composition engineering (e.g., keeping a high concentration of chalcogenide during the annealing process) and optimizing the chemical synthesis conditions to suppress the formation of deep-level defects (e.g., anion vacancies) or turn the deep-level defects into shallow defects through Ag or other cation alloying.

AUTHOR INFORMATION

Corresponding Authors

Xie Zhang − *School of Materials Science and Engineering, Northwestern Polytechnical University, Xi'an 710072, China;* orcid.org/0000-0003-3424-9253; Email: xie.zhang@nwpu.edu.cn

Chang Yan − *Sustainable Energy and Environment Thrust, Function Hub, Hong Kong University of Science and Technology (Guangzhou), Guangzhou 511453, China; Guangzhou Municipal Key Laboratory of Materials Informatics, Hong Kong University of Science and Technology (Guangzhou), Guangzhou 511453, China;* Email: changyan@hkust-gz.edu.cn

Authors

Xuan-Yan Chen − *Sustainable Energy and Environment Thrust, Function Hub, Hong Kong University of Science and Technology (Guangzhou), Guangzhou 511453, China;* orcid.org/0000-0002-7055-7387

Zihan Huang − *Sustainable Energy and Environment Thrust, Function Hub, Hong Kong University of Science and Technology (Guangzhou), Guangzhou 511453, China*

Zecheng Gan − *Advanced Materials Thrust, Function Hub, Guangzhou Municipal Key Laboratory of Materials Informatics and Guangzhou Municipal Key Laboratory of Materials Informatics, Hong Kong University of Science and Technology (Guangzhou), Guangzhou 511453, China;* orcid.org/0000-0002-7752-2136

Baoying Dou − *Henan Key Laboratory of Quantum Materials and Quantum Energy, School of Future Technology, Henan University, Zhengzhou 450046, China*

https://doi.org/10.1021/acs.jpcc.5c02431
J. Phys. Chem. C XXXX, XXX, XXX−XXX

Yan Wang − *Advanced Materials Thrust, Function Hub, Hong Kong University of Science and Technology (Guangzhou), Guangzhou 511453, China;* orcid.org/0009-0004-2585-750X

Complete contact information is available at: https://pubs.acs.org/10.1021/acs.jpcc.5c02431

Notes

The authors declare no competing financial interest.

■ ACKNOWLEDGMENTS

This work was supported by the National Natural Science Foundation of China (grant nos. 62204067, 52172136, and 12447180), the Young Talent Support Project of Guangzhou Association for Science and Technology (QT-2023-051), the Guangzhou Science and Technology Program (2023A03J0686), the Postdoctoral Fellowship Program of CPSF (grant no. GZC20240408), and industry support from Shenzhen Jinjia Jituan Co., Ltd. with funding No.R00043.

■ REFERENCES

(1) Saadat, M.; Moradi, M.; Zahedifar, M. CIGS absorber layer with double grading Ga profile for highly efficient solar cells. *Superlattices Microstruct.* **2016**, *92*, 303−307.

(2) Dullweber, T.; anna, G. H.; Rau, U.; Schock, H. W. A new approach to high-efficiency solar cells by band gap grading in $Cu(In,Ga)Se_2$ chalcopyrite semiconductors. *Sol. Energy Mater. Sol. Cells* **2001**, *67*, 145−150.

(3) Martin, N. M.; Törndahl, T.; Wallin, E.; Simonov, K. A.; Rensmo, H.; Platzer-Björkman, C. Surface/Interface Effects by Alkali Postdeposition Treatments of $(Ag,Cu)(In,Ga)Se_2$ Thin Film Solar Cells. *ACS Appl. Energy Mater.* **2022**, *5*, 461−468.

(4) Chirilă, A.; Reinhard, P.; Pianezzi, F.; Bloesch, P.; Uhl, A. R.; Fella, C.; Kranz, L.; Keller, D.; Gretener, C.; Hagendorfer, H.; et al. Potassium-induced surface modification of $Cu(In,Ga)Se_2$ thin films for high-efficiency solar cells. *Nat. Mater.* **2013**, *12*, 1107−1111.

(5) Siebentritt, S.; Avancini, E.; Bär, M.; Bombsch, J.; Bourgeois, E.; Buecheler, S.; Carron, R.; Castro, C.; Duguay, S.; Félix, R.; et al. Heavy Alkali Treatment of $Cu(In,Ga)Se_2$ Solar Cells: Surface versus Bulk Effects. *Adv. Energy Mater.* **2020**, *10*, 1903752.

(6) Raghuwanshi, M.; Vilalta-Clemente, A.; Castro, C.; Duguay, S.; Cadel, E.; Jackson, P.; Hariskos, D.; Witte, W.; Pareige, P. Influence of RbF post deposition treatment on heterojunction and grain boundaries in high efficient (21.1%) $Cu(In,Ga)Se_2$ solar cells. *Nano Energy* **2019**, *60*, 103−110.

(7) Nicoara, N.; Manaligod, R.; Jackson, P.; Hariskos, D.; Witte, W.; Sozzi, G.; Menozzi, R.; Sadewasser, S. Direct evidence for grain boundary passivation in $Cu(In,Ga)Se_2$ solar cells through alkali-fluoride post-deposition treatments. *Nat. Commun.* **2019**, *10*, 3980.

(8) Nakamura, M.; Yamaguchi, K.; Kimoto, Y.; et al. Cd-Free $Cu(In,Ga)(Se,S)_2$ Thin-Film Solar Cell With Record Efficiency of 23.35. *IEEE Journal of Photovoltaics* **2019**, *9*, 1863−1867.

(9) Keller, J.; Kiselman, K.; Donzel-Gargand, O.; et al. High-concentration silver alloying and steep back-contact gallium grading enabling copper indium gallium selenide solar cell with 23.6% efficiency. *Nat. Energy* **2024**, *9*, 467−478.

(10) Kim, K.; Ahn, S. K.; Choi, J. H.; Yoo, J.; Eo, Y.-J.; Cho, J.-S.; Cho, A.; Gwak, J.; Song, S.; Cho, D.-H.; et al. Highly efficient Ag-alloyed $Cu(In,Ga)Se_2$ solar cells with wide bandgaps and their application to chalcopyrite-based tandem solar cells. *Nano Energy* **2018**, *48*, 345−352.

(11) Chen, L.; Lee, J.; Shafarman, W. N. The Comparison of $(Ag,Cu)(In,Ga)Se_2$ and $Cu(In,Ga)Se_2$ Thin Films Deposited by Three-Stage Coevaporation. *IEEE Journal of Photovoltaics* **2014**, *4*, 447−451.

(12) Heyd, J.; Scuseria, G. E.; Ernzerhof, M. Hybrid functionals based on a screened Coulomb potential. *J. Chem. Phys.* **2003**, *118*, 8207−8215.

(13) Oikkonen, L. E.; Ganchenkova, M. G.; Seitsonen, A. P.; Nieminen, R. M. Vacancies in $CuInSe_2$: new insights from hybrid-functional calculations. *J. Phys.: Condens. Matter* **2011**, *23*, 422202.

(14) Dobrego, V. P.; Shlimak, I. S. The Influence of Local Potential Fluctuations on the Low-Temperature Radiative Recombination of Compensated Germanium. *physica status solidi (b)* **1969**, *33*, 805−809.

(15) Levanyuk, A. P.; Osipov, V. V. Edge luminescence of direct-gap semiconductors. *Soviet Physics Uspekhi* **1981**, *24*, 187−215.

(16) Teixeira, J. P.; Sousa, R. A.; Sousa, M. G.; Da Cunha, A. F.; Fernandes, P. A.; Salomé, P. M. P.; Leitão, J. P. Radiative transitions in highly doped and compensated chalcopyrites and kesterites: The case of Cu_2ZnSnS_4. *Phys. Rev. B* **2014**, *90*, 235202.

(17) Repins, I.; Mansfield, L.; Kanevce, A.; Jensen, S. A.; Kuciauskas, D.; Glynn, S.; Barnes, T.; Metzger, W.; Burst, J.; Jiang, C.-S. et al. Wild band edges: The role of bandgap grading and band-edge fluctuations in high-efficiency chalcogenide devices. *2016 IEEE 43rd Photovoltaic Specialists Conference (PVSC)*. 2016; pp 0309−0314.

(18) Abou-Ras, D.; Schäfer, N.; Hages, C. J.; Levcenko, S.; Márquez, J.; Unold, T. Inhomogeneities in $Cu(In,Ga)Se_2$ Thin Films for Solar Cells: Band-Gap Versus Potential Fluctuations. *Sol. RRL* **2018**, *2*, 1700199.

(19) Blöchl, P. E. Projector Augmented-Wave Method. *Phys. Rev. B* **1994**, *50*, 17953−17979.

(20) Kresse, G.; Furthmüller, J. Efficient iterative schemes for ab initio total-energy calculations using a plane-wave basis set. *Phys. Rev. B* **1996**, *54*, 11169−11186.

(21) Monkhorst, H. J.; Pack, J. D. Special points for Brillouin-zone integrations. *Phys. Rev. B* **1976**, *13*, 5188−5192.

(22) Boulkaddat, L.; Soussi, A.; Najih, H.; Abouabassi, K.; Ait hssi, A.; Labchir, N.; Elfanaoui, A.; Markazi, R.; Bouabid, K.; Ihlal, A. Experimental and theoretical study of electrodeposited $CuInS_2$ thin films for solar cell applications. *Phys. B* **2023**, *671*, 415374.

(23) Maeda, T.; Takeichi, T.; Wada, T. Systematic studies on electronic structures of $CuInSe_2$ and the other chalcopyrite related compounds by first principles calculations. *Physica Status Solidi (a)* **2006**, *203*, 2634−2638.

(24) Mustafa, H.; Hunter, D.; Pradhan, A. K.; Roy, U. N.; Cui, Y.; Burger, A. Synthesis and characterization of $AgInSe_2$ for application in thin film solar cells. *Thin Solid Films* **2007**, *515*, 7001−7004.

(25) Freysoldt, C.; Grabowski, B.; Hickel, T.; Neugebauer, J.; Kresse, G.; Janotti, A.; Van De Walle, C. G. First-principles calculations for point defects in solids. *Rev. Mod. Phys.* **2014**, *86*, 253−305.

(26) Freysoldt, C.; Neugebauer, J.; Van de Walle, C. G. Fully Ab Initio Finite-Size Corrections for Charged-Defect Supercell Calculations. *Phys. Rev. Lett.* **2009**, *102*, 016402.

(27) Liu, X.; Zhou, F.; Song, N.; Huang, J.; Yan, C.; Liu, F.; Sun, K.; Stride, J. A.; Hao, X.; Green, M. A. Exploring the application of metastable wurtzite nanocrystals in pure-sulfide Cu_2ZnSnS_4 solar cells by forming nearly micron-sized large grains. *J. Mater. Chem. A* **2015**, *3*, 23185−23193.

(28) Wei, S.-H.; Zhang, S. B. Defect properties of $CuInSe_2$ and $CuGaSe_2$. *J. Phys. Chem. Solids* **2005**, *66*, 1994−1999.

(29) Wei, S.-H.; Zhang, S. B.; Zunger, A. Effects of Ga addition to $CuInSe_2$ on its electronic, structural, and defect properties. *Appl. Phys. Lett.* **1998**, *72*, 3199−3201.

(30) Wei, S.-H.; Zhang, S. B.; Zunger, A. Effects of Na on the electrical and structural properties of $CuInSe_2$. *J. Appl. Phys.* **1999**, *85*, 7214−7218.

(31) Pohl, J.; Albe, K. Intrinsic point defects in $CuInSe_2$ and $CuGaSe_2$ as seen via screened-exchange hybrid density functional theory. *Phys. Rev. B* **2013**, *87*, 245203.

(32) Zhang, X.; Turiansky, M. E.; Van de Walle, C. G. Correctly Assessing Defect Tolerance in Halide Perovskites. *J. Phys. Chem. C* **2020**, *124*, 6022−6027.

(33) Zhang, X.; Turiansky, M. E.; Shen, J.-X.; Van de Walle, C. G. Iodine interstitials as a cause of nonradiative recombination in hybrid perovskites. *Phys. Rev. B* **2020**, *101*, 140101.
(34) Dou, B.; Falletta, S.; Neugebauer, J.; Freysoldt, C.; Zhang, X.; Wei, S.-H. Chemical Trend of Nonradiative Recombination in Cu (In, Ga) Se_2 Alloys. *Phys. Rev. Appl.* **2023**, *19*, 054054.
(35) Guo, H.; Yang, P.; Hu, J.; Jiang, A.; Chen, H.; Niu, X.; Zhou, Y. Band Structure Engineering and Defect Passivation of CuxAg1−xInS2/ZnS Quantum Dots to Enhance Photoelectrochemical Hydrogen Evolution. *ACS Omega* **2022**, *7*, 9642−9651.
(36) Sharan, A.; Sabino, F. P.; Janotti, A.; Gaillard, N.; Ogitsu, T.; Varley, J. B. Assessing the roles of Cu- and Ag-deficient layers in chalcopyrite-based solar cells through first principles calculations. *J. Appl. Phys.* **2020**, *127*, 065303.
(37) Maeda, T.; Wada, T. Electronic Structure and Characteristics of Chemical Bonds in CuInSe2, CuGaSe2, and CuAlSe2. *Jpn. J. Appl. Phys.* **2010**, *49*, 04DP07.
(38) Zhao, Y.; Yuan, S.; Kou, D.; Zhou, Z.; Wang, X.; Xiao, H.; Deng, Y.; Cui, C.; Chang, Q.; Wu, S. High Efficiency CIGS Solar Cells by Bulk Defect Passivation through Ag Substituting Strategy. *ACS Appl. Mater. Interfaces* **2020**, *12*, 12717−12726.
(39) Kato, T.; Wu, J.-L.; Hirai, Y.; Sugimoto, H.; Bermudez, V. Record Efficiency for Thin-Film Polycrystalline Solar Cells Up to 22.9% Achieved by Cs-Treated $Cu(In,Ga)(Se,S)_2$. *IEEE Journal of Photovoltaics* **2019**, *9*, 325−330.
(40) Yan, C.; Huang, J.; Sun, K.; Johnston, S.; Zhang, Y.; Sun, H.; Pu, A.; He, M.; Liu, F.; Eder, K.; et al. Cu_2ZnSnS_4 solar cells with over 10% power conversion efficiency enabled by heterojunction heat treatment. *Nat. Energy* **2018**, *3*, 764−772.
(41) Kiermasch, D.; Rieder, P.; Tvingstedt, K.; Baumann, A.; Dyakonov, V. Improved charge carrier lifetime in planar perovskite solar cells by bromine doping. *Sci. Rep.* **2016**, *6*, 39333.
(42) Lu, I.-T.; Zhou, J.-J.; Bernardi, M. Efficient ab initio calculations of electron-defect scattering and defect-limited carrier mobility. *Phys. Rev. Mater.* **2019**, *3*, 033804.

https://doi.org/10.1021/acs.jpcc.5c02431
J. Phys. Chem. C XXXX, XXX, XXX−XXX